Dynamic instability of microtubules requires dynamin 2 and is impaired in a Charcot-Marie-Tooth mutant

Kenji Tanabe and Kohji Takei

Department of Neuroscience, Okayama University Graduate School of Medicine, Dentistry, and Pharmaceutical Sciences, Okayama 700-8558, Japan

Dynamin is a fission protein that participates in endocytic vesicle formation. Although dynamin was originally identified as a microtubule-binding protein, the physiological relevance of this function was unclear. Recently, mutations in the ubiquitously expressed dynamin 2 (dyn2) protein were found in patients with Charcot-Marie-Tooth (CMT) disease, which is an inherited peripheral neuropathy. In this study, we show that one of these mutations, 551Δ3, induces prominent decoration of microtubules with the mutant dyn2. Dyn2 was required for proper dynamic instability of microtubules, and this was impaired in cells expressing the 551Δ3 mutant, which showed a remarkable increase in microtubule acetylation, a marker of stable microtubules. Depletion of endogenous dyn2 with a small interfering RNA also resulted in the accumulation of stable microtubules. Furthermore, the formation of mature Golgi complexes, which depends on microtubule-dependent membrane transport, was impaired in both dyn2 knockdown cells and cells expressing the 551Δ3 mutant. Collectively, our results suggest that dyn2 regulates dynamic instability of microtubules, which is essential for organelle motility, and that this function may be impaired in CMT disease.

Introduction

Dynamin was first identified as a microtubule-binding protein (Shpetner and Vallee, 1989, 1992; Scaife and Margolis, 1990; Maeda et al., 1992). However, the importance of its association with microtubules was questioned after the establishment of a function for dynamin in endocytosis. Dynamin is a homologue of the *Drosophila melanogaster shibire* gene (Chen et al., 1991), mutations in dynamin block endocytosis, and dynamin's GTPase activity is crucial for the fission of endocytic pits. Polymerized dynamin rings have been proposed to function as a pinchase (Urrutia et al., 1997) or poppase (Stowell et al., 1999) or by a molecular switch mechanism requiring subsequent activation of a downstream substrate (Sever et al., 2000).

Three dynamin isoforms have been identified in mammals. Dynamin 1 (dyn1) and dyn3 are tissue specific (neurons and brain for dyn1; testis, lung, and heart for dyn3), whereas dyn2 is ubiquitously expressed. Dynamin has five characteristic domains: a GTPase domain in its N terminus, a middle domain that binds to γ-tubulin; a pleckstrin homology (PH) domain that binds to phosphinositide-4,5-diphosphate and leads to membrane localization, a GTPase effector domain, and a pro-rich domain in the C terminus. The pro-rich domain binds to various SH3 domain–containing proteins and microtubules (Herskovits et al., 1993b).

Recently, dyn2 mutations were found to be associated with Charcot-Marie-Tooth (CMT) neuropathies (Zuchner et al., 2005), but the molecular and cellular mechanisms of dyn2's involvement in disease pathogenesis are still unclear. The CMT hereditary motor and sensory neuropathies fall into two main groups. CMT type 1 includes demyelinating forms of the disease in which nerve conduction velocities (NCVs) are reduced; CMT type 2 includes the axonal forms in which NCVs are normal, but conduction amplitudes are decreased (Suter and Scherer, 2003). There are also dominant intermediate (DI) subtypes of CMT, denoted DI-CMTA, DI-CMTB, and DI-CMTC, that are characterized by both axonal and demyelinating NCVs (Kennerson et al., 2001; Verhoeven et al., 2001;

Correspondence to Kohji Takei: kohji@md.okayama-u.ac.jp

Abbreviations used in this paper: CMT, Charcot-Marie-Tooth; DI, dominant intermediate; NAGT, *N*-acetylglucosaminyltransferase I; NCV, nerve conduction velocity; PH, pleckstrin homology.

The Rockefeller University Press $30.00
J. Cell Biol. Vol. 185 No. 6 939–948
www.jcb.org/cgi/doi/10.1083/jcb.200803153

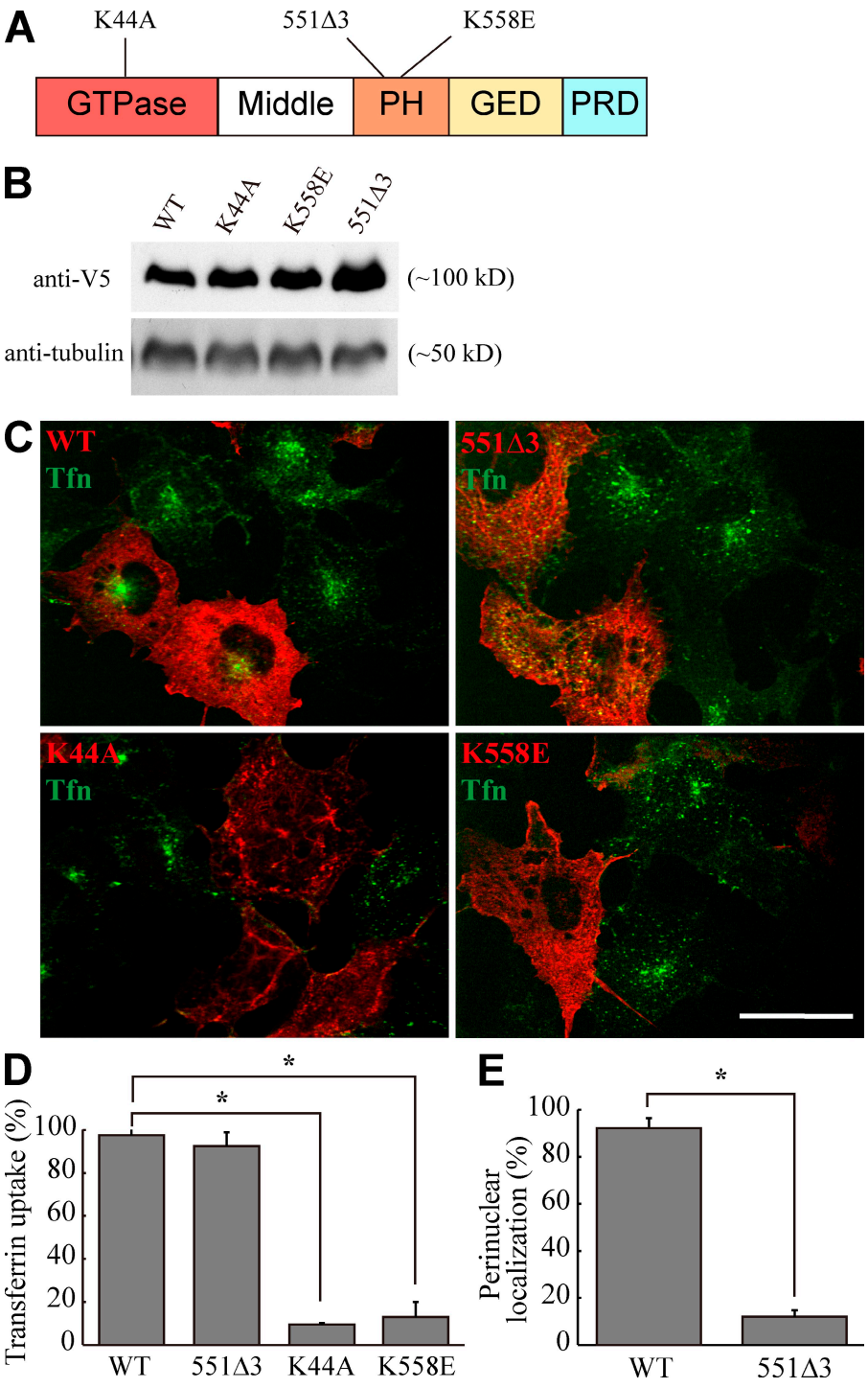

Figure 1. **Expression of the 551Δ3 dyn2 mutant does not inhibit transferrin endocytosis.** COS-7 cells were transfected with the indicated constructs and incubated with Alexa Fluor 488–transferrin for 30 min. (A) Schematic representation of dyn2 indicating functional domains and mutation sites used in this experiment. GED, GTPase effector domain. (B) The expression levels of exogenous proteins were confirmed by immunoblotting using anti-V5. (C) Confocal micrographs showing the subcellular distribution of internalized transferrin (Tfn; green) in transfected cells (red). (D) Quantification of the effect of the indicated constructs on transferrin internalization. The number of cells containing Alexa Fluor 488–transferrin is expressed relative to the total number of transfected cells. (E) Effect of the 551Δ3 dyn2 mutant on the perinuclear localization of internalized transferrin. The number of cells with perinuclear transferrin is expressed relative to the total number of transfected cells. Error bars indicate SD from two independent experiments; *, $P < 0.005$. WT, wild type. Bar, 20 µm.

Jordanova et al., 2003). DI-CMTB patients have mutations within the dyn2 PH domain, including the deletion mutant 551Δ3 and the point mutant K558E (Zuchner et al., 2005). This suggests that the impairment in CMT may be caused by an inability to form active dynamin polymers, which are needed to bind and then deform membranes to carry out peripheral cell functions (McNiven, 2005). In this study, we investigated the effect of the 551Δ3 mutation on dyn2 function and found that it induces the accumulation of stable microtubules, as does the reduction of endogenous dyn2, indicating that dyn2 regulates the dynamic instability of microtubules and that increased microtubule stability is one feature of CMT that is linked to mutations in dynamin.

Results and discussion

We assessed whether expression of the CMT-associated 551Δ3 and K558E dyn2 mutants inhibits endocytosis by transfecting COS-7 cells with dyn2 cDNAs and examining uptake of Alexa Fluor 488–transferrin. As a positive control, the cells were transfected with K44A, a GTPase-negative dyn2 mutant which is known to inhibit endocytosis (Herskovits et al., 1993a;

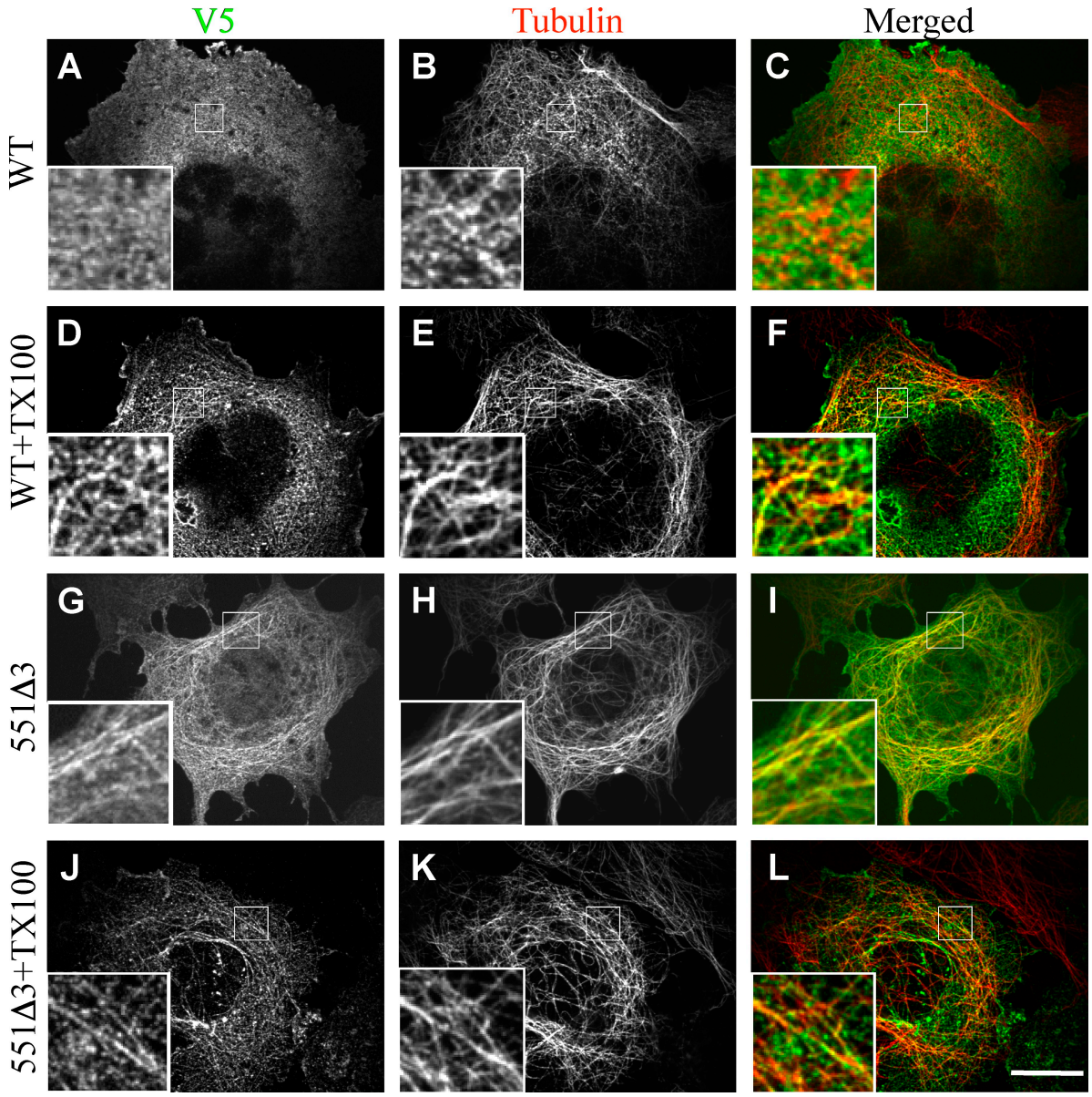

Figure 2. **Dyn2 remains associated with microtubules after the extraction of soluble proteins.** (A–L) COS-7 cells were transfected with the indicated constructs and incubated with antibodies specific for V5 (A, D, G, and J) or α-tubulin (B, E, H, and K), and the V5 and α-tubulin images were merged (C, F, I, and L). To extract the cytosolic proteins, the cells were incubated with Triton X-100 (TX100) before fixation and processed for immunofluorescence (D–F and J–L). The boxed areas are enlarged in the insets. WT, wild type. Bar, 10 μm.

van der Bliek et al., 1993). Although expression of either the K558E or K44A mutant completely blocked endocytosis (Fig. 1, A and B; Zuchner et al., 2005), expression of 551Δ3 did not (Fig. 1, A and B). However, the transferrin-containing compartments in the 551Δ3-transfected cells no longer accumulated at the perinuclear region (Fig. 1 C) but were instead transported to early and recycling endosomes (Fig. S1). Internalized transferrin-containing endosomes are transported along microtubules by dynein–dynactin complexes to perinuclear recycling endosomes (Burkhardt et al., 1997). Therefore, it is likely that processes involved in capturing endosomes or traveling along microtubules are impaired in 551Δ3-expressing cells. Supporting this microtubule-related role for dyn2, it has previously been shown that 551Δ3 expression induces microtubule reorganization (Zuchner et al., 2005). Moreover, dynamin was originally identified as a microtubule-associated protein (Shpetner and Vallee, 1989). Both dyn1 and dyn2 polymerize around microtubules, and these interactions lead to the stimulation of dynamin GTPase activity (Maeda et al., 1992; Warnock et al., 1997).

To test whether dyn2 localizes along microtubules, we transfected COS-7 cells with wild-type or 551Δ3 dyn2 cDNA constructs tagged with the V5 epitope. Microtubules were visualized by immunostaining for α-tubulin. Immunostaining with antibodies to V5 indicated that wild-type dyn2 was present in a punctate pattern on the plasma membrane as well as in substantial amounts in the cytosol, where the puncta seemed to colocalize with the microtubules (Fig. 2, A–C). 551Δ3 dyn2 also colocalized with and prominently decorated microtubules

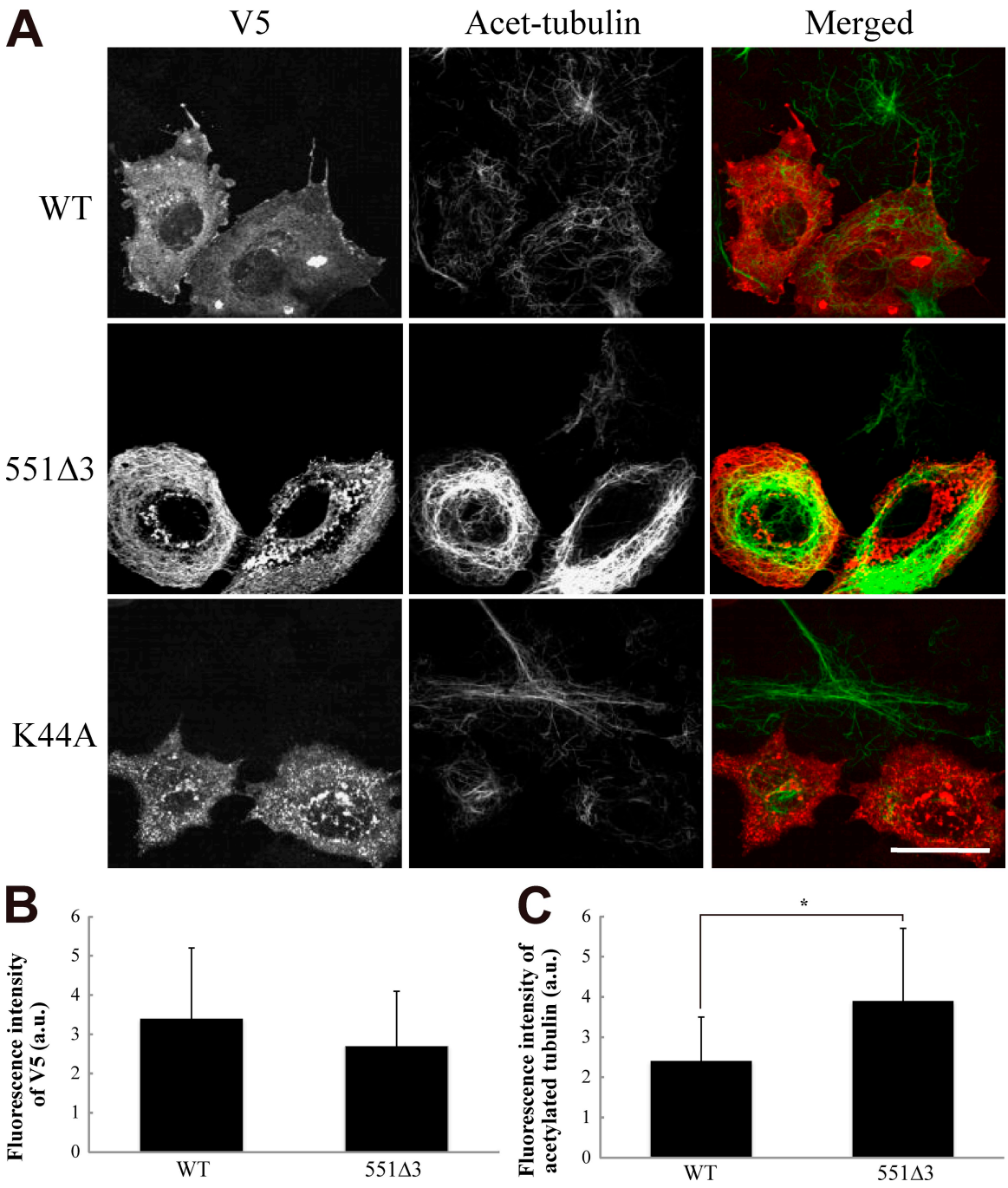

Figure 3. **Expression of the 551Δ3 dyn2 mutant causes the accumulation of acetylated tubulin.** (A) COS-7 cells were transfected with the indicated constructs, fixed 48 h later, and visualized with antibodies specific for V5 (red) and acetylated-tubulin (Acet-tubulin; green). (B and C) The expression level of V5-tagged proteins (B) and the level of acetylated tubulin against the V5 signals (C) were measured and averaged. Approximately 50 cells were used, and the data are represented in arbitrary units (a.u.). Error bars indicate SD; *, $P < 0.005$. WT, wild type. Bar, 20 µm.

(Fig. 2, G–I), as previously reported (Zuchner et al., 2005). To more clearly demonstrate the association of dyn2 with microtubules, we performed immunolocalization after cytosolic proteins were extracted from cells with Triton X-100. Both wild-type dyn2 (Fig. 2, D–F) and 551Δ3 (Fig. 2, J–L) clearly colocalized with the microtubules in these conditions (Zuchner et al., 2005). These results indicate that a subpopulation of dyn2 molecules localizes to microtubules in vivo and that the 551Δ3 mutation may alter the microtubule-binding properties of dyn2.

Taxol inhibits microtubule depolymerization and thus prevents normal dynamic instability (Green and Goldman, 1983). Therefore, we tested whether the dyn2 mutants could have the same effect. Acetylation distinguishes stable microtubules from dynamic microtubules (Piperno et al., 1987; Westermann and Weber, 2003), although tubulin acetylation itself does not promote microtubule stability (Palazzo et al., 2003). Accordingly, we assessed the effect of 551Δ3 expression in COS-7 cells on microtubule acetylation. Expression of wild-type, K44A, or

K558E dyn2 did not alter the degree of microtubule acetylation (Fig. 3 A and not depicted). In contrast, 551Δ3 expression resulted in a massive accumulation of acetylated tubulin (Fig. 3 A). Quantitative image analysis revealed a significant increase of acetylated tubulin in 551Δ3-expressing cells (the fluorescence intensity ratios of acetylated tubulin to dynamin-V5 were 3.9 ± 1.8 and 2.4 ± 1.1 in 551Δ3 and wild-type cells, respectively; $n = 30$, $P < 0.05$), with no significant difference in total tubulin expression between 551Δ3 and the wild type (Fig. 3, B and C). Thus, the differential microtubule-binding patterns observed in 551Δ3-expressing cells are likely caused by the abnormal accumulation of acetylated microtubules.

We then asked whether the 551Δ3-induced accumulation of acetylated microtubules is caused by a loss of function or a gain of function of dyn2. To this end, we examined the effect of siRNA-mediated depletion of endogenous dyn2 on microtubule stability in HeLa cells. Two different dyn2-specific siRNAs successfully knocked down endogenous dyn2 in HeLa cells (Fig. S2), and transferrin internalization was inhibited (not depicted), as reported previously (Huang et al., 2004). Immunofluorescence of the dyn2 siRNA–treated (dyn2 siRNA) cells did not show any apparent reorganization of microtubules (Fig. 4 A). However, Western blot and immunofluorescence analyses revealed that these cells had an approximately twofold increase in acetylated tubulin, although the total tubulin protein levels did not change (Fig. 4, A and B). In addition, localization of EB1 to the plus end of dynamic/growing microtubules in control siRNA–treated cells (Mimori-Kiyosue and Tsukita, 2003) was significantly reduced in dyn2 siRNA cells (Fig. 4 A and Fig. S2, D and E), whereas total EB1 protein levels were unchanged (Fig. 4 B). In contrast, the minus ends of microtubules were not affected by the siRNA treatment, as judged by staining pericentrin (Fig. 4 A) or γ-tubulin (not depicted). These results indicate that depletion of endogenous dyn2, like the 551Δ3 mutant, induces the accumulation of acetylated microtubules and reduces the proportion of dynamic/growing microtubules. Thus, the 551Δ3-induced accumulation of stable microtubules is caused by a loss of microtubule-related dyn2 function.

To further confirm the effect of dyn2 depletion on microtubule stability, we performed the following two experiments. First, we treated siRNA-transfected HeLa cells with nocodazole, which is an inhibitor of microtubule polymerization. As the half life of stable microtubules (∼1 h) is much longer than that of dynamic microtubules (∼5–10 min; Schulze et al., 1987), nocodazole is expected to be more effective on dynamic microtubules. Nocodazole treatment for up to 1 h resulted in the disappearance of microtubules in control cells, whereas microtubules persisted in dyn2 siRNA cells (Fig. 4, C and D). Next, we analyzed the effect of dyn2 siRNA on HeLa cells that stably express GFP-tubulin. In control cells, microtubules showed repeated growth and shrinkage, a behavior known as dynamic instability (Mitchison and Kirschner, 1984), whereas growth and shrinkage were less frequently observed in dyn2 siRNA cells (Fig. 4 E and Video 1). Thus, dyn2 depletion indeed induces stable microtubule accumulation. Analysis of various microtubule dynamic instability parameters in dyn2 siRNA cells revealed that neither the growth rate nor the shortening rate was significantly changed by dyn2 depletion (Table I). This indicates that dyn2 depletion does not affect the microtubule polymerization or depolymerization mechanisms but rather increases the duration of microtubule pause. This implies that wild-type dyn2 increases the frequency of microtubule growth and/or shrinkage.

Next, we investigated how the effect of dyn2 on microtubules contributes to cellular activities. Because impaired dynamic instability of microtubules is suggested to inhibit trafficking along microtubules (Mimori-Kiyosue and Tsukita, 2003; Vaughan, 2005) and Golgi apparatus formation is dependent on microtubule-mediated transport (Thyberg and Moskalewski, 1999), we examined Golgi formation in dyn2 siRNA cells and 551Δ3-expressing cells. External tracers could not be used to directly monitor microtubule-dependent transport in these experiments because they cannot be internalized by the dyn2 siRNA cells (Thyberg and Moskalewski, 1999). As expected, the Golgi complex was dispersed in ∼90% of dyn2 siRNA cells (Fig. 5 A, left). The fragments of the Golgi complex maintained characteristic cisternal stack morphologies, as judged with double-immunofluorescence staining using cis/medial (GRASP65)- and trans (p230)-Golgi markers (Fig. 5 A, right) and with electron microscopy (Fig. 5 B).

To rule out the possibility that the Golgi fragmentation in dyn2 siRNA cells is an indirect effect of endocytotic blockade, we analyzed Golgi formation in the 551Δ3-expressing cells, in which dyn-dependent endocytosis is not blocked (Fig. 1). As controls, we also examined Golgi formation in K44A- and K558E-expressing cells, in which endocytosis is blocked (Fig. 1). Unlike expression of either K44A or K558E, 551Δ3 expression induced Golgi fragmentation (Fig. S3). Thus, the Golgi fragmentation in dyn2 siRNA cells is not caused by the inhibition of dynamin-dependent endocytosis but is more likely the result of impaired organelle transport, which is dependent on normal microtubule dynamic instability. The regulation of microtubule stability by dyn2 seems to be independent of its GTPase activity because the K44A mutant had no effect on microtubule-dependent organelle transport (Fig. S3 B). Similarly, the role of dyn2 in centrosome cohesion does not require its GTP domain (Thompson et al., 2004). Therefore, it is possible that dyn2 can function as a structural protein independently of its GTPase activity.

How is microtubule-dependent transport impaired by dyn2 depletion or expression of the 551Δ3 mutation? One possibility is that minus end–oriented motor proteins are inhibited in these cells. Supporting this, inhibition of these motor proteins has been observed when dynamitin, a subunit of the dynein–dynactin complex, is overexpressed (Burkhardt et al., 1997). Alternatively, dyn2 depletion and 551Δ3 expression may impair the capture of pre-Golgi intermediates onto microtubules. To examine these two possibilities, we analyzed the movement of the fragmented Golgi in dyn2-depleted HeLa cells. For this purpose, HeLa cells expressing *N*-acetylglucosaminyltransferase I (NAGT)–GFP, a Golgi marker, were transfected with different dyn2 siRNA constructs, and Golgi fragmentation was induced by nocodazole treatment. The nocodazole was then washed out to allow microtubule polymerization, and the movement of the fragmented Golgi during the recovery phase was observed by live cell imaging. In control cells, the fragmented Golgi eventually moved

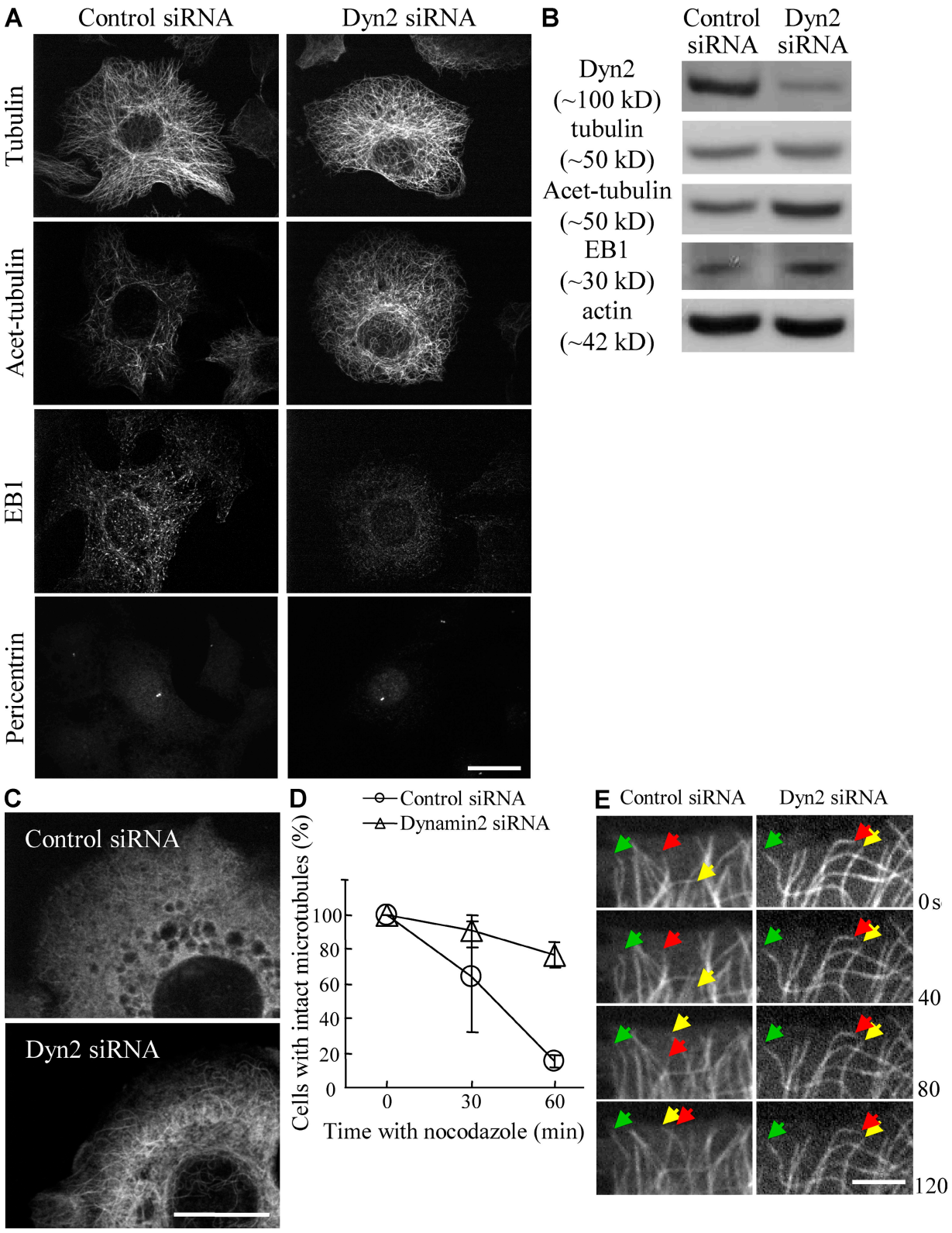

Figure 4. **Depletion of endogenous dyn2 by RNAi results in stable microtubule accumulation.** HeLa cells were transfected with control or dyn2-specific siRNA. (A) Immunofluorescence of RNAi-treated cells. The cells were fixed and visualized with antibodies specific for α-tubulin, acetylated tubulin (Acet-tubulin), EB1, and pericentrin. (B) Western blot analysis of the cells transfected with control or dyn2 siRNA. The blots were visualized with the indicated antibodies. (C and D) Dyn2 siRNA–treated cells are resistant to nocodazole treatment. The cells were incubated with nocodazole for 30 or 60 min and then fixed and visualized with anti–α-tubulin. The images in C show the cells after 30 min of nocodazole treatment. In D, the cells with intact microtubules are expressed relative to the total number of cells. The results represent the mean ± SD from two independent experiments. (E) The microtubules are less dynamic in dyn2 siRNA–treated cells. HeLa cells stably expressing GFP-tubulin were transfected with control or dyn2 siRNA, and images were collected every 2 s. Representative microtubules are indicated by arrows. Bars: (A and C) 10 µm; (E) 2 µm.

Table I. **Microtubule dynamic instability parameters**

Parameters	Control siRNA	Dyn2 siRNA
Rate of growth (μm/min)	10.1 ± 6.7	7.9 ± 4.6
Rate of shortening (μm/min)	14.1 ± 9.8	11.6 ± 8.8
Duration of growth (%)	4.2	1.7
Duration of pause (%)	89.7	98.6
Duration of shortening (%)	6.1	0.9

17 and 20 events were measured for control and dyn2 siRNA, respectively, and SD is shown.

toward the perinuclear region (Fig. 5 C and Video 2). However, in dyn2 siRNA cells, we did not observe perinuclear concentration of the fragmented Golgi, even after 30 min. Furthermore, tracking analysis revealed that movement of the fragmented Golgi in control siRNA cells repeatedly stopped (Fig. 5 C), which might reflect a search and capture behavior (Vaughan, 2005). However, in the dyn2 siRNA cells, such movement was rarely seen. Moreover, although the velocity of the fragmented Golgi in dyn2 siRNA cells was comparable with that of control cells (Fig. 5 D), the total distance moved was reduced in the dyn2 siRNA cells (Fig. 5 E). These results suggest that, although movement along microtubules was not altered by dyn2 depletion, microtubule-mediated capture was inhibited. Because pre-Golgi elements are captured by interacting with EB1, which localizes on microtubule plus ends (Vaughan, 2005), the dyn2 depletion–mediated reduction of EB1 recruitment (Fig. 4 A) may be responsible for the fragmentation of the Golgi complex. In dyn2 siRNA cells, EB1 was no longer localized in a punctate manner at the plus ends of microtubules, whereas the protein level was not affected (Fig. 4, A and B), demonstrating that dyn2 knockdown caused dislocation of EB1 from microtubule plus ends to the cytosol. It is unlikely that dyn2 directly acts on EB1 because dyn2 is localized along the entire length of the microtubules rather than restricted to the plus ends. However, it is plausible that the mislocalization of EB1 in dyn2 siRNA cells is a consequence of altered microtubule stability.

To date, dynamin has been found to function in vesicle fission in endocytosis (Takei et al., 1995), in actin reorganization (Schafer, 2004), and in centrosome cohesion (Thompson et al., 2004). This study reveals yet another function, namely in dynamic instability of microtubules. We showed that this function of dyn2 is essential for microtubule-dependent membrane transport. It is unlikely that the accumulation of stable microtubules and the fragmentation of the Golgi apparatus are caused by dysfunction of the centrosome (Thompson et al., 2004) because we did not detect impairment of the centrosome in the dyn2 siRNA–transfected HeLa cells (Fig. 4 A). Decreased microtubule instability might impair capture of pre-Golgi organelles, which is necessary for the formation of the mature Golgi. Alternatively, dynamin might be involved in the maintenance of cargo attachment to the microtubules. Further examination is required to distinguish between these possibilities.

In this study, we demonstrated that different CMT mutants affect different membrane transport events. Thus, K558E affects endocytosis, whereas 551Δ3 impairs microtubule-dependent transport (Fig. 3). This is consistent with observations that suggest neuropathies, including CMT, are caused by defects in membrane transport steps such as endocytosis, axonal transport, or protein degradation (Suter and Scherer, 2003). Notably, all of the dyn2 mutations that are associated with CMT, including 551Δ3 and K558E, are located in the PH domain (Zuchner et al., 2005). The predicted structures of these mutant PH domains indicate that 551Δ3 but not K558E impairs the proper formation of the β3/β4 loops, which is required for dyn2 dimerization. This implies that the decoration of microtubules induced by 551Δ3, not by dyn2 depletion, may be caused by the abnormal polymerization activity of 551Δ3 resulting from the loss of dyn2 dimerization. In other words, wild-type dyn2 may contribute to the correct bundling of microtubules through its polymerization activity. Interestingly, dynamin was identified previously as a microtubule-binding protein (Shpetner and Vallee, 1989) that cross-links microtubules to form bundles in vitro (Scaife and Margolis, 1990; Maeda et al., 1992; Shpetner and Vallee, 1992). Dynamin also increases its GTPase activity when it polymerizes around microtubules (Warnock et al., 1997). However, the physiological significance of these observations was unclear. This study is the first indication that dyn2 plays a role in the regulation of dynamic instability of microtubules in vivo and that this function of dyn2 is essential for microtubule-dependent membrane transport. However, the fact that dyn2 localizes at the microtubule bundle in cytokinesis (Thompson et al., 2002) and at the centrosome (Thompson et al., 2004) implies it has even more diverse microtubule-related functions, the elucidation of which will also require further study.

Materials and methods

Reagents and antibodies

All chemicals and reagents were of biochemical grade. Nocodazole was purchased from Sigma-Aldrich. The following primary antibodies were used: rabbit antibodies against V5 (Millipore), pericentrin (Covance), and GRASP65 (a gift from N. Nakamura, Kanazawa University, Kanazawa, Japan); mouse antibodies against GM130, EB1, and p230 (BD); α-tubulin, β-actin, and acetylated tubulin (Sigma-Aldrich); and goat anti-dyn2 (Santa Cruz Biotechnology, Inc.). The following secondary antibodies were used: Alexa Fluor 488–conjugated anti–goat IgG and Rhodamine red-X–conjugated anti–mouse IgG (Invitrogen); Cy3-conjugated anti–rat IgG (KPL); and HRP-conjugated anti–mouse IgG, anti–rabbit IgG, and anti–goat IgG (Thermo Fisher Scientific). Alexa Fluor 488–conjugated human transferrin was also purchased from Invitrogen.

DNA construction

Wild-type and K44A mutant rat dyn2 cDNAs were a gift from M. McNiven (Mayo Clinic, Rochester, MN) and were subcloned into pcDNA4 V5/His (Invitrogen). Mutations were introduced with QuikChange II XL (Agilent Technologies) in accordance with the manufacturer's instructions, and sequences were verified by DNA sequencing. NAGT-GFP was a gift from N. Nakamura, and GFP-Rab5 and -Rab11 were gifts from M. Fukuda (Tohoku University, Sendai, Japan). DNA was purified for transfection experiments by using a Plasmid Maxi kit from QIAGEN.

Cell culture and transfection

COS-7 and HeLa cells were maintained in DME supplemented with 10% serum. Transfection was performed by using Effectene (QIAGEN) according to the manufacturer's instructions. The cells were analyzed 48 h after transfection. The uptake of transferrin was performed by incubating the cells with 25 μg/ml Alexa Fluor 488–conjugated transferrin for 30 min at 37°C, as described previously (Tanabe et al., 2005). Detergent extraction experiments were performed by incubating the cells in Brinkley reassembly buffer (BRB80; 80 mM Pipes/KOH, pH 6.8, 4% polyethylene glycol 8000,

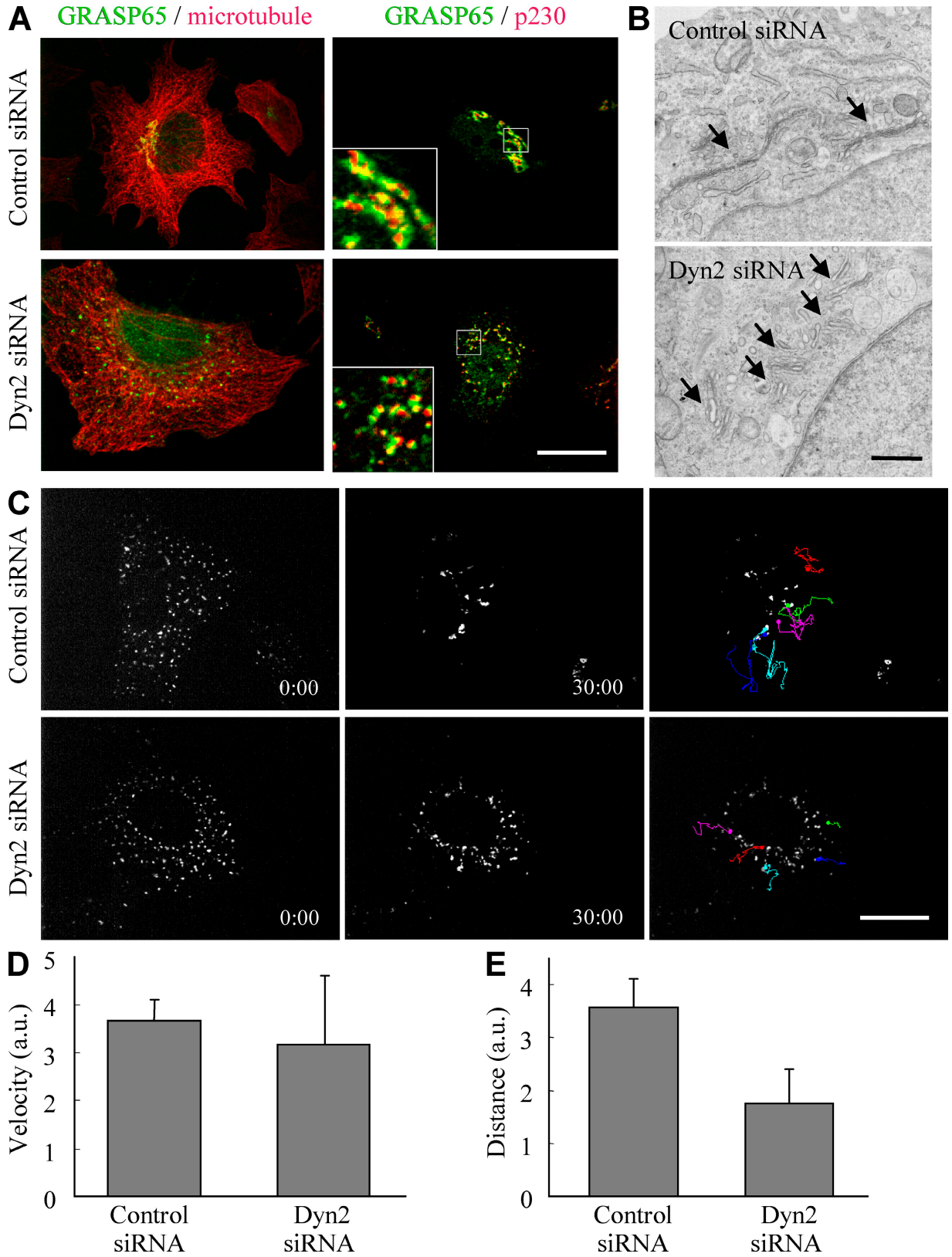

Figure 5. **Dyn2 is required for the formation of the Golgi complex but not for transport along microtubules.** (A) Dyn2 siRNA–treated cells show fragmented Golgi but maintain their stacks. HeLa cells were transfected with the indicated siRNAs and visualized with antibodies specific for GRASP65 (green) and α-tubulin or p230 (red). The boxed areas are enlarged in the insets. (B) Electron micrographs show the Golgi stacks (arrows) in the siRNA-transfected cells. (C) HeLa cells expressing NAGT-GFP were transfected with the indicated siRNAs and treated with nocodazole for 2 h. The cells were then washed and incubated in the absence of nocodazole. Images were collected every 3 s for 30 min. The signals were tracked manually, and representative tracks are shown in different colors. (D and E) The velocity (D) and distance moved (E) by 15 fragments in three cells for each siRNA were measured and averaged. The data are represented in arbitrary units (a.u.). The results represent the mean ± SD. Bars: (A and C) 10 µm; (B) 2 µm.

1 mM $MgCl_2$, and 1 mM EGTA) containing 1% Triton X-100 for 10 min at 37°C (Royle et al., 2005). The cells were washed once with BRB80 without Triton X-100, fixed with 3.7% formaldehyde, and processed for immunofluorescence analysis.

RNAi

Human dyn2–specific siRNAs (dyn2 siRNA 1, 5′-GGAUAUUGAGGGCAAGAAG-3′; and dyn2 siRNA 2, 5′-GCGAAUCGUCACCACUUAC-3′) were purchased from Applied Biosystems, as was the negative control siRNA. The siRNAs were introduced into HeLa cells by using Lipofectamine 2000 (Invitrogen) according to the manufacturer's instructions. The cells were analyzed at the indicated times after transfection. For Western blot analysis, the cells were lysed in SDS-PAGE sample buffer, boiled for 5 min, subjected to SDS-PAGE, and transferred to nitrocellulose membranes. The blots were then incubated overnight at 4°C in blocking buffer (140 mM NaCl, 1 mM EDTA, and 20 mM Tris-HCl, pH 7.4) containing 5% skim milk and 0.02% Tween 20 followed by incubation for 1 h at room temperature first with primary antibodies and then with secondary antibodies diluted in blocking buffer. The proteins were visualized by using enhanced chemiluminescence (GE Healthcare).

Immunofluorescence and electron microscopy

Cells were fixed with 3.7% formaldehyde in PBS for 15 min at room temperature or with 100% methanol for 10 min at −20°C. After three washes with PBS, the cells were treated with 1% BSA and 0.1% Triton X-100 in PBS for 30 min and then incubated with primary antibodies for 45 min at room temperature. After three washes with PBS, the cells were incubated for 30 min at room temperature with secondary antibodies. After another three washes with PBS, the cells were mounted in PermaFluor (Thermo Fisher Scientific) and analyzed by the spinning disc confocal microscope system (CSU10; Yokogawa Electric Co.) on an inverted microscope (IX-71; Olympus) equipped with an Ar/Kr laser. Images were acquired using a UPlan-Apochromat 100× NA 1.35 oil immersion objective (Olympus) and an electron-multiplying charge-coupled device camera (iXon; Andor Technology). Image capture and acquisition were performed using MetaMorph software (MDS Analytical Technologies). All images were saved as TIFF files, and brightness and contrast were adjusted with ImageJ software (National Institutes of Health). For conventional electron microscopy, cells were fixed with 4% paraformaldehyde and 2% glutaraldehyde in 0.1 M phosphate buffer, pH 7.4, for 10 min at room temperature. The series were observed by using a transmission electron microscope (H-7100; Hitachi) at the Central Research Laboratory at the Okayama University Medical School.

Live imaging and data analysis

HeLa cells stably expressing GFP–α-tubulin were a gift from Y. Mimori-Kiyosue (Knowledge Action Network Research Institute, Kobe, Japan). To visualize the Golgi complex, NAGT-GFP was introduced into HeLa cells by Effectene. The cells were transfected with siRNAs 24 h after DNA transfection and then observed 48 h later. To observe Golgi motility, the cells were incubated with 10 µM nocodazole for 2 h and then washed and incubated in DME + 10% FBS. The cells were incubated in culture medium and kept at 37°C and 5% CO_2 using a stage incubator (MI-IBC; Olympus) and digital gas mixer (GM-2000; Tokai Hit) and imaged using the aforementioned confocal system. The quantification and analysis of fluorescent signals was performed by using MetaMorph software and ImageJ. Microtubule dynamic instability parameters were measured as described previously (Shelden and Wadsworth, 1993; Mimori-Kiyosue et al., 2005). In brief, HeLa cells stably expressing GFP–α-tubulin were imaged with a 2-s interval 72 h after transfection with siRNAs. Life history plots of 17 microtubules in three control cells and 20 microtubules in four dyn2 siRNA cells were analyzed. The duration of growth/pause/shrinking of microtubules was analyzed as described in Shelden and Wadsworth (1993). Rates of growth/shrinking are instantaneous (measured within one interval between successive frames). All data were analyzed for significance using a Student's *t* test.

Online supplemental material

Fig. S1 shows localization of internalized transferrin under the expression of the 551Δ3 mutant. Fig. S2 shows the dyn2 siRNA effects on acetylated tubulin and EB1 localization. Fig. S3 shows Golgi fragmentation induced by the expression of 551Δ3. Videos 1 and 2 show time-lapse experiments of HeLa cells stably expressing GFP–α-tubulin or NAGT-GFP, respectively, that were transfected with control or dyn2 siRNAs.

We thank Dr. Mark McNiven for the dyn2 constructs, Dr. Nobuhiro Nakamura for the anti-GRASP65 antibody and NAGT-GFP construct, Dr. Yuko Mimori-Kiyosue for the GFP–α-tubulin–expressing cells, and Dr. Mitsunori Fukuda for the GFP-Rab constructs.

This work was supported by a Grant-in-Aid for Scientific Research from the Ministry of Education, Culture, Sports, Science and Technology of Japan.

Submitted: 28 March 2008
Accepted: 15 May 2009

References

Burkhardt, J.K., C.J. Echeverri, T. Nilsson, and R.B. Vallee. 1997. Overexpression of the dynamitin (p50) subunit of the dynactin complex disrupts dynein-dependent maintenance of membrane organelle distribution. *J. Cell Biol.* 139:469–484.

Chen, M.S., R.A. Obar, C.C. Schroeder, T.W. Austin, C.A. Poodry, S.C. Wadsworth, and R.B. Vallee. 1991. Multiple forms of dynamin are encoded by shibire, a *Drosophila* gene involved in endocytosis. *Nature*. 351:583–586.

Green, K.J., and R.D. Goldman. 1983. The effects of taxol on cytoskeletal components in cultured fibroblasts and epithelial cells. *Cell Motil.* 3:283–305.

Herskovits, J.S., C.C. Burgess, R.A. Obar, and R.B. Vallee. 1993a. Effects of mutant rat dynamin on endocytosis. *J. Cell Biol.* 122:565–578.

Herskovits, J.S., H.S. Shpetner, C.C. Burgess, and R.B. Vallee. 1993b. Microtubules and Src homology 3 domains stimulate the dynamin GTPase via its C-terminal domain. *Proc. Natl. Acad. Sci. USA*. 90:11468–11472.

Huang, F., A. Khvorova, W. Marshall, and A. Sorkin. 2004. Analysis of clathrin-mediated endocytosis of EGF receptor by RNA interference. *J. Biol. Chem.* 279:16657–16661.

Jordanova, A., F.P. Thomas, V. Guergueltcheva, I. Tournev, F.A. Gondim, B. Ishpekova, E. De Vriendt, A. Jacobs, I. Litvinenko, N. Ivanova, et al. 2003. Dominant intermediate Charcot-Marie-Tooth type C maps to chromosome 1p34-p35. *Am. J. Hum. Genet.* 73:1423–1430.

Kennerson, M.L., D. Zhu, R.J. Gardner, E. Storey, J. Merory, S.P. Robertson, and G.A. Nicholson. 2001. Dominant intermediate Charcot-Marie-Tooth neuropathy maps to chromosome 19p12-p13.2. *Am. J. Hum. Genet.* 69:883–888.

Maeda, K., T. Nakata, Y. Noda, R. Sato-Yoshitake, and N. Hirokawa. 1992. Interaction of dynamin with microtubules: its structure and GTPase activity investigated by using highly purified dynamin. *Mol. Biol. Cell*. 3:1181–1194.

McNiven, M.A. 2005. Dynamin in disease. *Nat. Genet.* 37:215–216.

Mimori-Kiyosue, Y., and S. Tsukita. 2003. "Search-and-capture" of microtubules through plus-end-binding proteins (+TIPs). *J. Biochem.* 134:321–326.

Mimori-Kiyosue, Y., I. Grigoriev, G. Lansbergen, H. Sasaki, C. Matsui, F. Severin, N. Galjart, F. Grosveld, I. Vorobjev, S. Tsukita, and A. Akhmanova. 2005. CLASP1 and CLASP2 bind to EB1 and regulate microtubule plus-end dynamics at the cell cortex. *J. Cell Biol.* 168:141–153.

Mitchison, T., and M. Kirschner. 1984. Dynamic instability of microtubule growth. *Nature*. 312:237–242.

Palazzo, A., B. Ackerman, and G.G. Gundersen. 2003. Cell biology: Tubulin acetylation and cell motility. *Nature*. 421:230.

Piperno, G., M. LeDizet, and X.J. Chang. 1987. Microtubules containing acetylated alpha-tubulin in mammalian cells in culture. *J. Cell Biol.* 104:289–302.

Royle, S.J., N.A. Bright, and L. Lagnado. 2005. Clathrin is required for the function of the mitotic spindle. *Nature*. 434:1152–1157.

Scaife, R., and R.L. Margolis. 1990. Biochemical and immunochemical analysis of rat brain dynamin interaction with microtubules and organelles in vivo and in vitro. *J. Cell Biol.* 111:3023–3033.

Schafer, D.A. 2004. Regulating actin dynamics at membranes: a focus on dynamin. *Traffic*. 5:463–469.

Schulze, E., D.J. Asai, J.C. Bulinski, and M. Kirschner. 1987. Posttranslational modification and microtubule stability. *J. Cell Biol.* 105:2167–2177.

Sever, S., H. Damke, and S.L. Schmid. 2000. Dynamin:GTP controls the formation of constricted coated pits, the rate limiting step in clathrin-mediated endocytosis. *J. Cell Biol.* 150:1137–1148.

Shelden, E., and P. Wadsworth. 1993. Observation and quantification of individual microtubule behavior in vivo: microtubule dynamics are cell-type specific. *J. Cell Biol.* 120:935–945.

Shpetner, H.S., and R.B. Vallee. 1989. Identification of dynamin, a novel mechanochemical enzyme that mediates interactions between microtubules. *Cell*. 59:421–432.

Shpetner, H.S., and R.B. Vallee. 1992. Dynamin is a GTPase stimulated to high levels of activity by microtubules. *Nature*. 355:733–735.

Stowell, M.H., B. Marks, P. Wigge, and H.T. McMahon. 1999. Nucleotide-dependent conformational changes in dynamin: evidence for a mechanochemical molecular spring. *Nat. Cell Biol.* 1:27–32.

Suter, U., and S.S. Scherer. 2003. Disease mechanisms in inherited neuropathies. *Nat. Rev. Neurosci.* 4:714–726.

Takei, K., P.S. McPherson, S.L. Schmid, and P. De Camilli. 1995. Tubular membrane invaginations coated by dynamin rings are induced by GTP-gamma S in nerve terminals. *Nature*. 374:186–190.

Tanabe, K., T. Torii, W. Natsume, S. Braesch-Andersen, T. Watanabe, and M. Satake. 2005. A novel GTPase-activating protein for ARF6 directly interacts with clathrin and regulates clathrin-dependent endocytosis. *Mol. Biol. Cell*. 16:1617–1628.

Thompson, H.M., A.R. Skop, U. Euteneuer, B.J. Meyer, and M.A. McNiven. 2002. The large GTPase dynamin associates with the spindle midzone and is required for cytokinesis. *Curr. Biol.* 12:2111–2117.

Thompson, H.M., H. Cao, J. Chen, U. Euteneuer, and M.A. McNiven. 2004. Dynamin 2 binds gamma-tubulin and participates in centrosome cohesion. *Nat. Cell Biol.* 6:335–342.

Thyberg, J., and S. Moskalewski. 1999. Role of microtubules in the organization of the Golgi complex. *Exp. Cell Res.* 246:263–279.

Urrutia, R., J.R. Henley, T. Cook, and M.A. McNiven. 1997. The dynamins: redundant or distinct functions for an expanding family of related GTPases? *Proc. Natl. Acad. Sci. USA*. 94:377–384.

van der Bliek, A.M., T.E. Redelmeier, H. Damke, E.J. Tisdale, E.M. Meyerowitz, and S.L. Schmid. 1993. Mutations in human dynamin block an intermediate stage in coated vesicle formation. *J. Cell Biol.* 122:553–563.

Vaughan, K.T. 2005. Microtubule plus ends, motors, and traffic of Golgi membranes. *Biochim. Biophys. Acta*. 1744:316–324.

Verhoeven, K., M. Villanova, A. Rossi, A. Malandrini, P. De Jonghe, and V. Timmerman. 2001. Localization of the gene for the intermediate form of Charcot-Marie-Tooth to chromosome 10q24.1-q25.1. *Am. J. Hum. Genet.* 69:889–894.

Warnock, D.E., T. Baba, and S.L. Schmid. 1997. Ubiquitously expressed dynamin-II has a higher intrinsic GTPase activity and a greater propensity for self-assembly than neuronal dynamin-I. *Mol. Biol. Cell*. 8:2553–2562.

Westermann, S., and K. Weber. 2003. Post-translational modifications regulate microtubule function. *Nat. Rev. Mol. Cell Biol.* 4:938–947.

Zuchner, S., M. Noureddine, M. Kennerson, K. Verhoeven, K. Claeys, P. De Jonghe, J. Merory, S.A. Oliveira, M.C. Speer, J.E. Stenger, et al. 2005. Mutations in the pleckstrin homology domain of dynamin 2 cause dominant intermediate Charcot-Marie-Tooth disease. *Nat. Genet.* 37:289–294.